CONCEPTS OF FEEDER DESIGN AND PERFORMANCE IN RELATION TO LOADING BULK SOLIDS ONTO CONVEYOR BELTS

Alan W. Roberts.

Emeritus Professor and Director,
Centre for Bulk Solids and Particulate Technologies,
The University of Newcastle, NSW 2308. Australia.

SUMMARY

This paper presents an overview of the concepts of feeder design in relation to the loading of bulk solids onto belt conveyors. The basic design features of belt and apron feeders is presented. The need for feeders and mass-flow hoppers to be designed as an integral unit to promote uniform feed is emphasised. The essential requirement is to promote uniform feed with the whole of the hopper/feeder interface active. The methods for determining feeder loads and corresponding drive torques and powers are discussed. Procedures for controlling feeder loads during start-up and running are explained. The estimation of loads on feeders used in conjunction with funnel-flow, expanded-flow bins and gravity reclaim stockpiles is discussed. The design of feed chutes for directing the flow of bulk solids from the feeder discharge onto conveyor belts is briefly reviewed.

1. INTRODUCTION

Feeders have an important function in belt conveying operations. Their function is to control the gravity flow of bulk solids from storage, such as from bins or stockpiles, and to provide a uniform feedrate to the receiving belt conveyor. While there are several types of feeders commonly used, it is important that they be chosen to suit the particular bulk solid and to provide the range of feed rates required. It is also important that feeders be used in conjunction with mass-flow hoppers to ensure both reliable flow and good control over the feeder loads and drive powers. Correct interfacing of feeders and hoppers is essential if performance objectives such uniform draw of material over the whole of the hopper outlet is to be achieved.

For uniform draw with a fully active hopper outlet, the capacity of the feeder must progressively increase in the direction of feed. In the case of a screw feeder, for example, this is achieved by using combinations of variable pitch, screw and core or shaft diameter. In the case of belt and apron feeders, a tapered opening is required as illustrated in Figure 1. The triangular skirtplates in the hopper bottom are an effective way to achieve the required taper. The gate on the front of the feeder is a flow trimming device and not a flow rate controller. The height of the gate is adjusted to give the required release angle and to achieve uniform draw along the slot. Once the gate is correctly adjusted, it should be fixed in position; flow rate is then controlled by varying the speed of the feeder. An alternative arrangement is to use a diverging front skirt or brow as illustrated in Figure 1. This has the advantage of relieving the pressure at the feed end during discharge and forward flow.

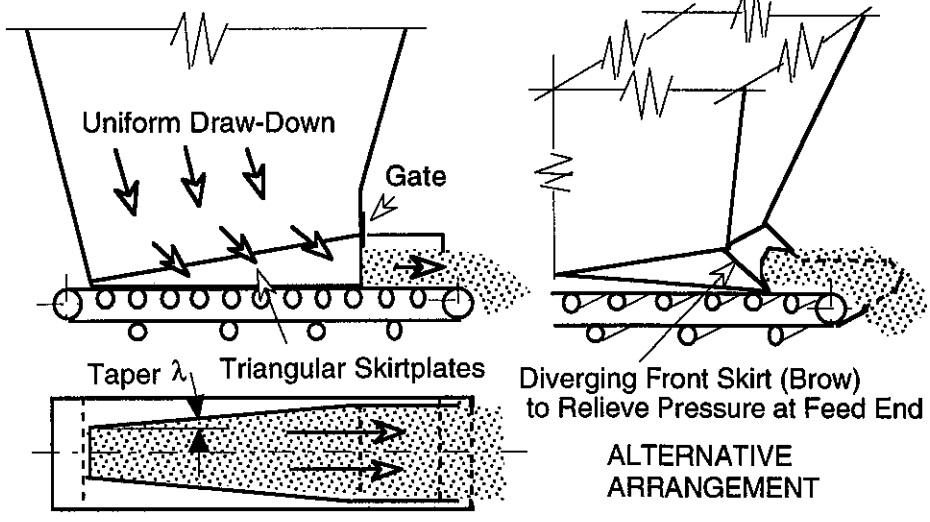

Figure 1. Belt or Apron Feeder

In the case of vibratory feeders, there is a tendency for feed to occur preferentially from the front. To overcome this problem, it is recommended that the slope angle of the front face of the hopper be increased by 5^{o} to 8^{o} as illustrated in Figure 2. Alternatively, the lining surface of the front face in the region of the outlet may selected so as to have a higher friction angle than the other faces. Apart from providing flexible support, the springs in the support rods or cables assist in controlling feeder loads. This is discussed later.

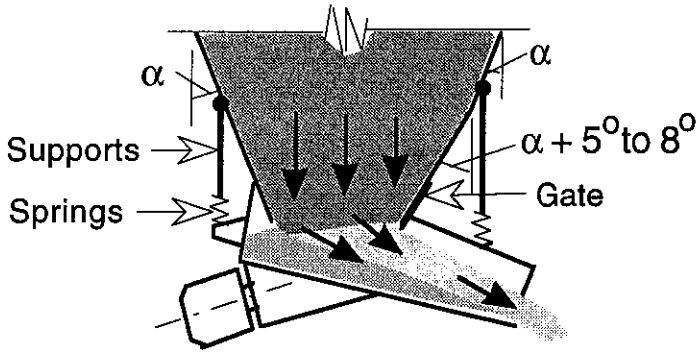

Figure 2. Vibratory Feeder

2. FEEDER LOADS DURING FILLING AND FLOW

2.1 General Remarks

From a design point of view, it is important to be able to determine the loads acting on feeders in hopper/feeder combinations and the corresponding power requirements. Figure 3 illustrates the loads acting in a hopper and feeder.

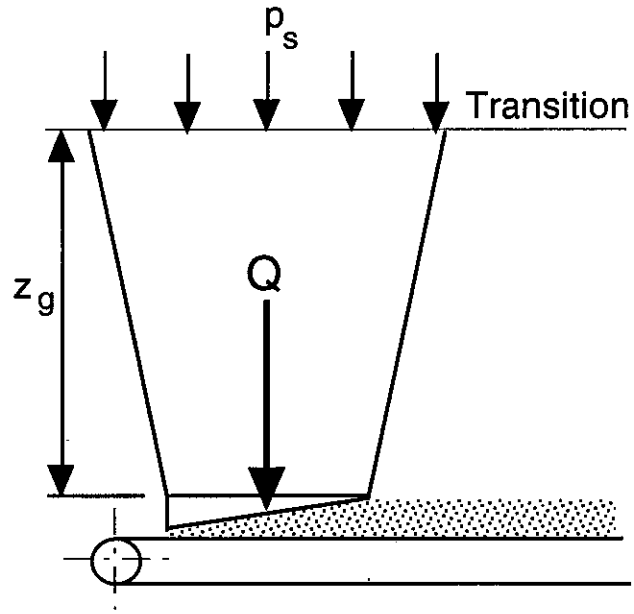

Figure 3. Feeder Loads in Hopper/Feeder Combination

Feeder loads are influenced by several factors including

- Hopper/feeder flow pattern
- Flow properties of the bulk solid
- The chosen hopper shape for mass-flow. That is, whether conical, plane-flow or transition (combination of conical and plane-flow).
- Wall friction characteristics between the bulk solid and hopper walls and skirtplates
- The type of feeder and its geometrical proportions

- The stress field established in the hopper. That is the initial filling condition when the hopper is filled from the empty condition and the flow condition when discharge has occurred.

For the initial filling condition in the case of a mass-flow hopper, the load is influenced by the surcharge pressure p_s acting at the hopper transition. For the flow condition, the load on the feeder is virtually independent of the surcharge head. This gives rise to a significant decrease in the feeder load Q once flow has been initiated.

Reisner [1] indicated that the initial load on a feeder may be 2 to 4 times the flow load. However, research has shown that variations between the initial and flow loads can be much greater than those indicated by Reisner.

2.2 Measurement of Feeder Loads

Experiments were conducted by Roberts et al [2] and Manjunath et al [3] using a laboratory scale plane-flow bin and belt feeder. The belt feeder was suspended by vertical wires attached to load cells to permit measurement of the feeder loads. The vertical wires were adjustable to permit setting the feeder to a chosen inclination or declination angle. Horizontal restraining wires, also attached to load cells, permitted measurement of the tangential force to move the bulk solid by means of the belt. The feeder was driven by a variable speed hydraulic motor, the motor being mounted for torque measurement.

A typical set of feeder load results for the filling and discharge conditions is shown in Figure 4. The graphs show the vertical initial and flow loads and the corresponding tangential loads. The variation between the initial filling and flow loads is quite significant, the flow load being only 18% of the initial load.

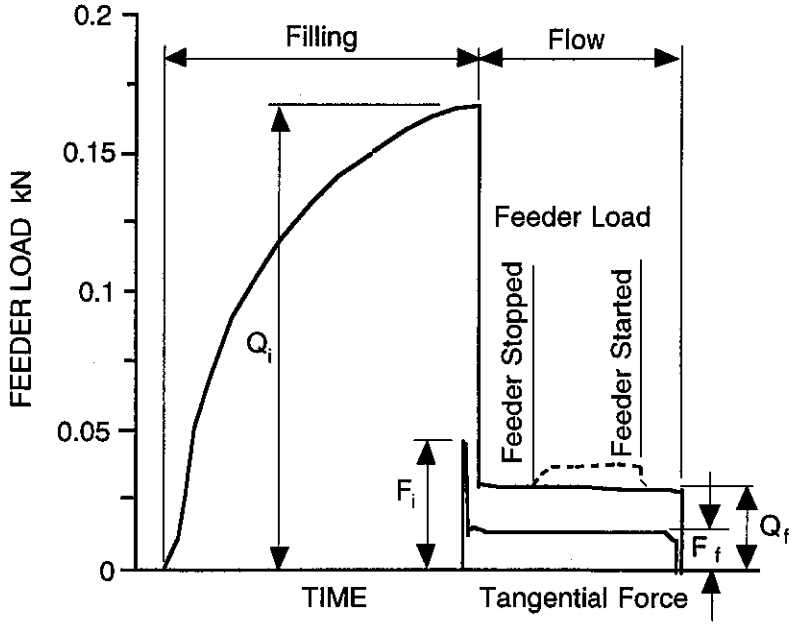

Figure 4. Feeder Loads for Belt Feeder Test Rig
Bin: D = 0.53 m, B = 0.06 m; $\alpha = 15^o$; L = 0.69 m; H = 0.5 m
Material: Plastic Pellets $\delta = 42^o$; $\phi = 20^o$; $\rho = 0.485$ t/m^3

It is also important to note that once flow has been initiated and then the feeder is stopped while the bin is still full, the load on the feeder does not revert to the original initial load. Rather, the load remains essentially at the flow load Q_f. The results of Figure 4 indicates a small increase in the load shown by the 'dotted' graph., this being no doubt due to a redistribution of the stress field in the region of the hopper outlet. Often, even this small increase does not occur.

The reduction in the tangential load from the initial value F_i to the flow value F_f in this case is about 60%. It is also noted that $\frac{F_i}{Q_i} = 0.27$ and $\frac{F_f}{Q_f} = 0.5$.

3. STRESS FIELDS IN HOPPER - INFLUENCE ON FEEDER LOADS

3.1 Pressures generated in a Mass-Flow Bin

In hopper and feeder combinations, the loads acting on the feeders are related to the pressures acting in the mass-flow hoppers. The vertical pressure p_{vo} at the outlet is of particular interest since this pressure directly influences the load on the feeder. This is illustrated in Figure 5.

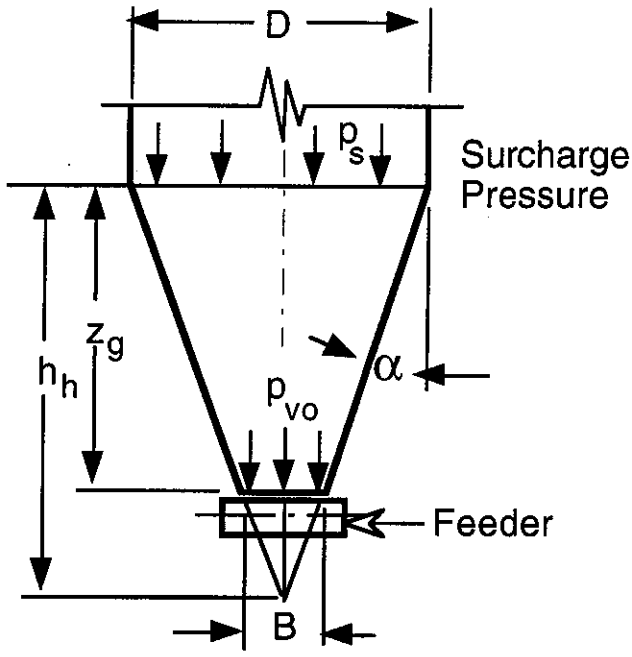

Figure 5. Pressures Acting in Hopper and Feeder

The stress fields are depicted in Figure 6 where p_n represents the normal wall pressure and p_v the average vertical pressure at the cross-section considered.

Under initial filling conditions, a peaked stress field is generated throughout the entire bin as illustrated in Figure 6 (a). Once flow is initiated, an arched stress field is generated in the hopper and a much greater proportion of the bulk solid load is supported by the upper section of the hopper walls. Consequently, the load acting on the feeder substantially reduces.

The variation of feeder loads illustrated in Figure 4 is explained by the change in pressure p_{vo} from the 'initial filling' to the 'flow' case by reference to Figure 6. It is noted that the pressures p_{vo} depicted in Figure 6 are influenced by a re-distribution of the stress field at the hopper outlet in the region of the feeder. It is also noted that the arched stress field in the hopper, once generated, is quite stable and is retained even when the feeder is stopped. This explains why when flow is initiated and then the feeder is stopped while the bin is still full, the arched stress field is retained and the load on the feeder remains at the reduced value.

3.2 Expressions for Pressures Acting in Mass-Flow Hopper

Since the design equations for feeder loads are related to the expressions for bin wall loads, notably the pressures generated in hoppers, the basic equations for mass-flow hoppers are briefly reviewed.

(a) General Expression

The vertical pressure

$$p_{vh} = \gamma\left[\frac{h_h - z_h}{j - 1}\right] + \left[\left(p_s - \frac{\gamma h_h}{(j - 1)}\right)\left(\frac{h_h - z_h}{h_h}\right)^j\right] \qquad (1)$$

$$p_{nf} = k_{hf}\, p_{vf} \qquad (2)$$

where $$j = (m+1)\left\{k_h\left(1 + \frac{\tan\phi_w}{\tan\alpha}\right) - 1\right\} \qquad (3)$$

α = hopper half angle
p_s = surcharge pressure at datum transition
h_h = distance from apex to transition
γ = bulk specific weight
ϕ_w = wall friction angle.
m = symmetry factor
= 1 for axi-symmetric or conical hoppers
= 0 for plane-flow hoppers

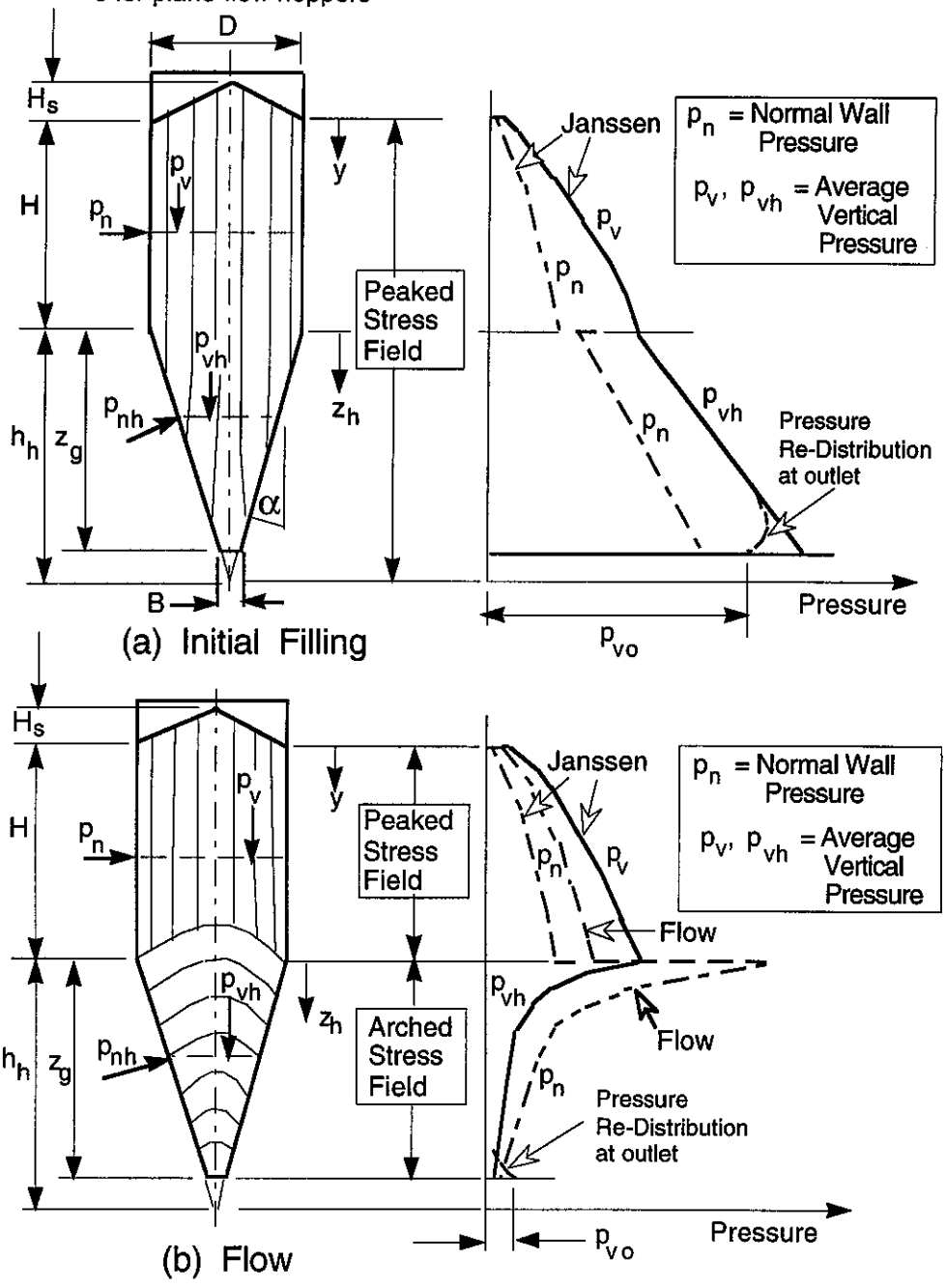

Figure 6. Pressures Acting in Mass-Flow Bin

(b) Hopper Pressures - Initial Filling Case

For the initial filling case, the minimum value of k_h (that is, k_{hi}), is used. For this case, j = 0 and the vertical pressure p_{vhi} is hydrostatic. From equation (1), with j = 0,

$$p_{vhi} = p_s + \gamma z_h \tag{4}$$

and the normal pressure p_{nhi} is

$$p_{nhi} = k_{hi}\, p_{vhi} = k_{hi}\,(p_s + \gamma z_h) \tag{5}$$

and from (3) with j = 0,

$$k_{hi} = \frac{\tan\alpha}{\tan\phi_w + \tan\alpha} \tag{6}$$

(c) Hopper Pressures - Flow Case

Equations (1) and (2) apply. That is

$$p_{vhf} = \gamma\left[\frac{h_h - z_h}{j - 1}\right] + \left[\left(p_s - \frac{\gamma h_h}{(j-1)}\right)\left(\frac{h_h - z_h}{h_h}\right)^j\right] \tag{7}$$

$$p_{nhi} = k_{hi}\, p_{vhf} \tag{8}$$

and

$$j = (m+1)\left\{k_{hf}\left(1 + \frac{\tan\phi_w}{\tan\alpha}\right) - 1\right\} \tag{9}$$

$$k_{hf} = \frac{2\,(1 + \sin\delta\cos2\eta)}{2 - \sin\delta\,(1 + \cos2(\alpha + \eta))} \tag{10}$$

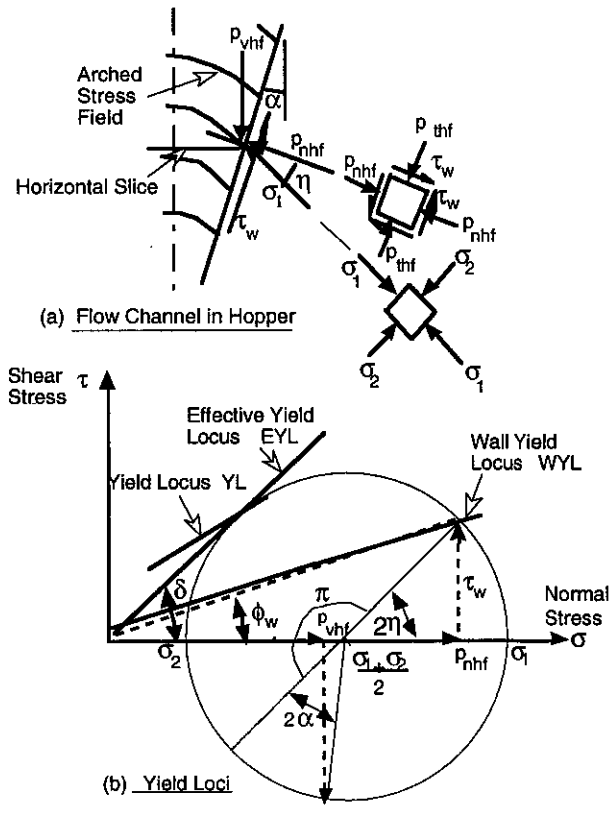

Figure 7. Stress or Pressure Conditions in Hopper during Flow

The stress or pressure conditions acting in the flow channel and corresponding Mohr circle representation are shown in Figure 7. The stress ratio k_{hf} relates the average vertical stress across the horizontal 'slice' to the normal pressure at the wall. As shown in Ref.[5], recommended value of k_{hf} is given by

4. DETERMINATION OF FEEDER LOADS - DESIGN EQUATIONS

4.1 General Case

Consider the mass-flow hopper and feeder of Figure 12. The design equations used to determine the feeder loads are summarised below:

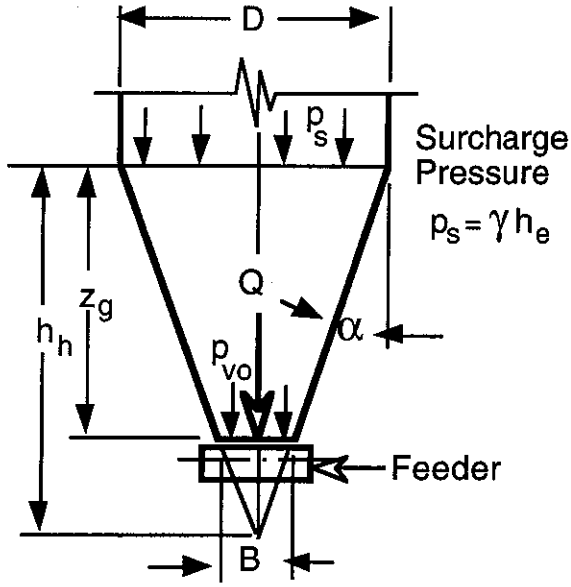

Figure 8 - Loads on Feeder

The loads acting on the feeder and corresponding power requirements vary according to the stress condition in the stored bulk mass.

The general expression for the load Q is

$$Q = p_{vo} A_o \qquad (11)$$

Where p_{vo} = Vertical pressure on feeder surface
A_o = Area of hopper outlet

For convenience, following the procedure established by Arnold et al [4], the load may be expressed in terms of a non-dimensional surcharge factor as follows:

$$Q = q \gamma B^{(2+m)} L^{(1+m)} \qquad (12)$$

Where q = non-dimensional surcharge factor
γ = ρ g = bulk specific weight
ρ = bulk density
L = length of slotted opening
B = width of slot or diameter of circular opening
m = hopper symmetry factor
m = 0 for plane-flow hopper
m = 1 for conical hopper

It follows from (11) and (12) that

$$q = \left(\frac{\pi}{4}\right)^m \frac{p_{vo}}{g\,B} \qquad (13)$$

Based on an analysis of the pressure distribution in the hopper, it may be shown that the vertical pressure acting at the hopper outlet is

$$p_{vo} = \frac{\gamma B}{2\,(j-1)\tan\alpha} + \left[p_s - \frac{\gamma D}{2\,(j-1)\tan\alpha}\right]\left[\frac{B}{D}\right]^j \qquad (14)$$

where p_s = surcharge pressure acting at the transition

The exponent 'j' in equation (20) is given by

$$j = (m+1)\left[k_h\left(1 + \frac{\tan\phi_w}{\tan\alpha} - 1\right]\right. \qquad (15)$$

where k_h is the ratio of normal pressure at the hopper wall to the corresponding average vertical pressure.

From (19) and (20) a general expression for the non-dimensional surcharge pressure may be obtained. That is,

$$q = \left(\frac{\pi}{4}\right)^m \left\{\frac{1}{2\,(j-1)\tan\alpha} + \left[\frac{p_s}{\gamma D} - \frac{1}{2\,(j-1)\tan\alpha}\right]\left[\frac{B}{D}\right]^{j-1}\right\} \qquad (16)$$

Two cases are of importance, the initial filling condition and the flow condition.

4.2 Initial Filling Condition

This applies when the feed bin is initially empty and then filled while the feeder is not operating. Research has shown that the initial filling loads can vary substantially according to such factors as

(i) Rate of filling and height of drop of solids as may produce impact effects.

(ii) Uniformity of filling over the length and breadth of the feed bin; asymmetric loading will produce a non-uniform pressure distribution along the feeder.

(iii) Clearance between the hopper bottom and feeder surface.

(iv) Degree of compressibility of bulk solid

(v) Rigidity of feeder surface

For the initial filling condition, the stress field in the hopper is peaked; that is, the major principal stress is almost vertical at any location. The determination of the initial surcharge factor q_i can be made by using an appropriate value of 'j' in equation (16). The following cases are considered:

(a) For a totally incompressible bulk solid and a rigid feeder with minimum clearance, the upper bound value of q_i may be approached. The upper bound value corresponds to $j = 0$ for which the vertical pressure in the hopper is 'hydrostatic'. In this case the ratio of normal pressure to vertical pressure is given by

$$k_{hi} = \frac{\tan\alpha}{\tan\alpha + \tan\phi_w} \qquad (17)$$

With $j = 0$, the upper bound value of q_i is obtained from equation (6) which becomes

$$q_i = \left(\frac{\pi}{4}\right)^m \left\{\frac{1}{2\tan\alpha}\left[\frac{D}{B} + \frac{2\,p_s\tan\alpha}{\gamma B} - 1\right]\right\} \qquad (18)$$

This equation corresponds to the pressure at the outlet being 'hydrostatic'.

(b) For a very incompressible bulk solid and a stiff feeder, j = 0.1

(c) For a very compressible bulk solid and a flexibly supported feeder, j = 0.9

(d) For a moderately compressible bulk solid stored above a flexibly supported feeder, j = 0.45

While the value of q_i may be determined using an appropriate value of j in equation (22), from a practical point of view, it has been established that a satisfactory prediction of q_i may be obtained from

$$q_i = \left(\frac{\pi}{4}\right)^m \left\{\frac{1}{2 \tan \alpha}\left[\frac{D}{B} + \frac{2\, p_s \tan \alpha}{\gamma D} - 1\right]\right\} \qquad (19)$$

The vertical load Q_i is given by

$$Q_i = q_i\ \rho\ g\ L^{(1-m)}\ B^{(2+m)} \qquad (20)$$

4.3 Flow Condition

Once flow has been initiated, an arched stress field is set up in the hopper. Even if the feeder is started and then stopped, the arched stress field in the hopper is preserved. In this case, the hopper is able to provide greater wall support and the load on the feeder, together with the corresponding drive power, is significantly reduced. While equation (16) may be applied by choosing an appropriate value of 'j', some difficulty arises due to the redistribution of stress that occurs at the hopper/feeder interface. A well established procedure, based on Jenike's radial stress theory has been presented in Refs.[2,3,5]. This procedure has some shortcomings inasmuch as the influence of the surcharge pressure p_s, although small, is ignored and while the hopper half-angle is included in the analysis, the aspect ratio $\frac{B}{D}$ of the hopper is not taken into account. An alternative approach is now presented.

The redistribution of the stress field in the clearance space between the hopper and the feeder is illustrated in Figure 9.

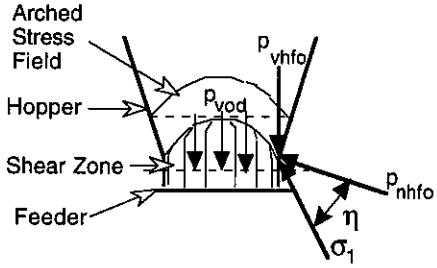

Figure 9. Stress Fields at Hopper and Feeder Interface

In this case the stress field in the shear zone is assumed to be peaked with the vertical design pressure p_{vod} being equal to the major consolidation pressure σ_1 determined by assuming that the average vertical pressure p_{vhf} at the hopper outlet is equal to mean principal consolidation pressure. This gives rise to the pressure multiplier k_{Fm} defined as follows:

$$k_{Fm} = (m + 1)(1 + \sin \delta) \qquad (21)$$

m = 0 for plane-flow
m = 1 for axi-symmetric or conical hoppers

Hence $p_{vod} = k_{Fm}\, p_{vhf}$ (22)

p_{vhfo} is given by equation (14). Hence

$$p_{vod} = k_{Fm}\left\{\frac{\gamma B}{2 (j - 1) \tan \alpha} + \left[p_s - \frac{\gamma D}{2 (j - 1) \tan \alpha}\right]\left[\frac{B}{D}\right]^j\right\} \qquad (23)$$

where $$j = (m+1)\left\{k_{hf}\left(1 + \frac{\tan\phi_w}{\tan\alpha}\right) - 1\right\} \quad (24)$$

and

$$k_{hf} = \frac{2\,(1 + \sin\delta\cos 2\eta)}{2 - \sin\delta\,(1 + \cos 2(\alpha + \eta))} \quad (25)$$

The force acting at the outlet and is

$$Q_f = p_{vod}\, A_o \quad (26)$$

where $$A_o = \text{Area of outlet} = \left(\frac{\pi}{4}\right)^m D^{(m+1)}\, L^{(1-m)} \quad (27)$$

Alternatively, the non-dimensional surcharge factor q_f is obtained from equation (13)

$$q_f = \left(\frac{p}{4}\right)^m \frac{p_{vod}}{\gamma B} \quad (28)$$

Combining (23) and (28)

$$q = k_{Fm}\left(\frac{\pi}{4}\right)^m \left\{\frac{1}{2\,(j-1)\tan\alpha} + \left[\frac{p_s}{\gamma D} - \frac{1}{2\,(j-1)\tan\alpha}\right]\left[\frac{B}{D}\right]^{j-1}\right\} \quad (29)$$

$$Q_f = q_f\, \rho\, g\, L^{(1-m)}\, B^{(2+m)} \quad (30)$$

4.4 Experimental Results

Figure 10 shows a comparison between the predicted and experimental results for the feeder test rig described in Refs.[2,3]. The flow load has been adjusted to allow for the weight of bulk material in the shear and extended skirtplate zones. In general, the results are in reasonable agreement.

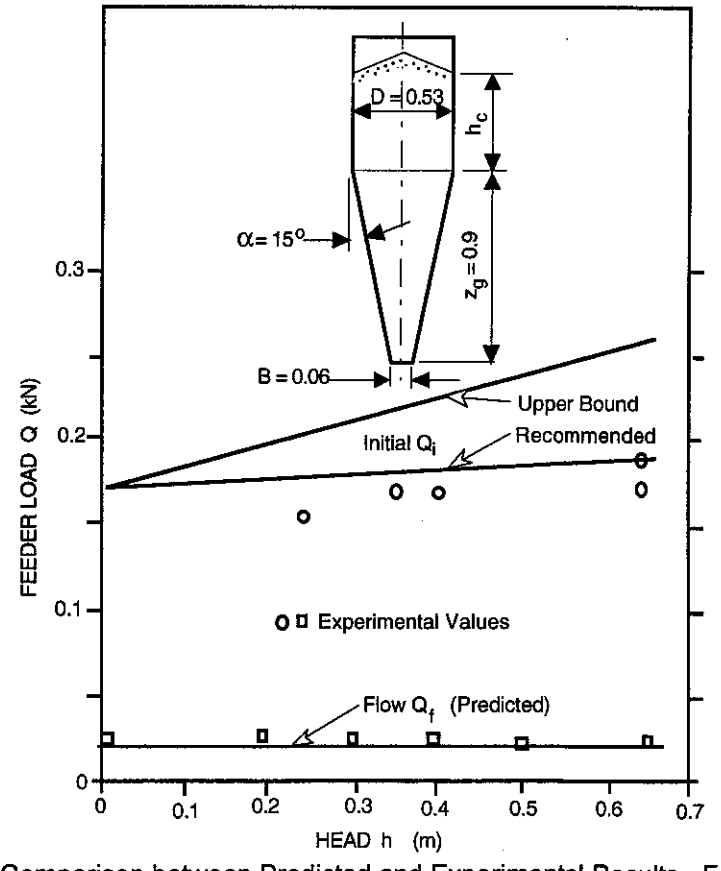

Figure 10. Comparison between Predicted and Experimental Results - Feeder Test Rig
Bulk Material: Plastic Pellets

5. BELT AND APRON FEEDERS

5.1 Shear Zone

The geometry of the shear zone of a belt or apron feeder is quite difficult to predict precisely. According to Schulze and Schwedes [6], the shear zone may be divided into three regions as illustrated in Figure 11. In their work the lengths of the regions were predicted on the basis of the 'Coulomb principle of smallest safety' which assumes that the rupture surface in a consolidated bulk solid will develop in such a way that the bearing capacity of the solid is minimised.

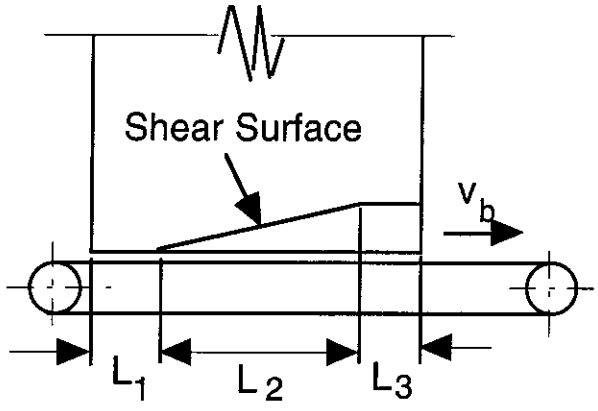

Figure 11. Shear Zones in Belt Feeder - Schulze et al [6]

It is also noted that there will be a velocity gradient developed in the shear zone, as indicated in Figure 12. The characteristic shape of this profile depends on the properties of the bulk solid, the feeder speed and the geometry of the hopper/feeder interface. In the extended skirtplate zone the velocity distribution is more uniform.

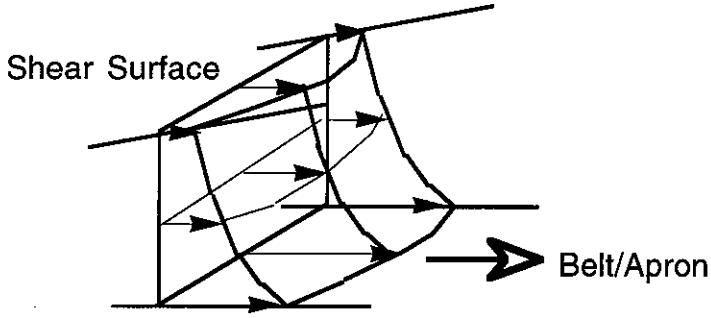

Figure 12. Velocity Profile in Shear Zone

The 'idealised' shear zone and velocity profiles are shown in Figure 13. For simplicity, it is reasonable to assume that the shear zone is linear and is defined by the release angle y. It is also assumed that in the shear zone the velocity profile is linear as illustrated in Figure 13. In the extended skirtplate zone, the velocity profile is substantially constant with the bulk solid moving at a average velocity equal to the belt velocity. Since the average bulk solid velocity in the hopper skirtplate zone is less than the average velocity in the extended skirtplate zone, there will be a 'vena contracta' effect with the bed depth y_e less than the bed depth H at the exit end of the feeder.

5.2 Release Angle

The height of the opening at the feed end should be sufficient to give an acceptable release angle ψ for controlled draw-down in the hopper and to avoid slip between the bulk solid and the belt or apron surface. At the same time the bed depth in the skirtplate zone should be selected to ensure uniform feed. It is recommend that

$$\frac{H}{B} \leq 1.0 \qquad (31)$$

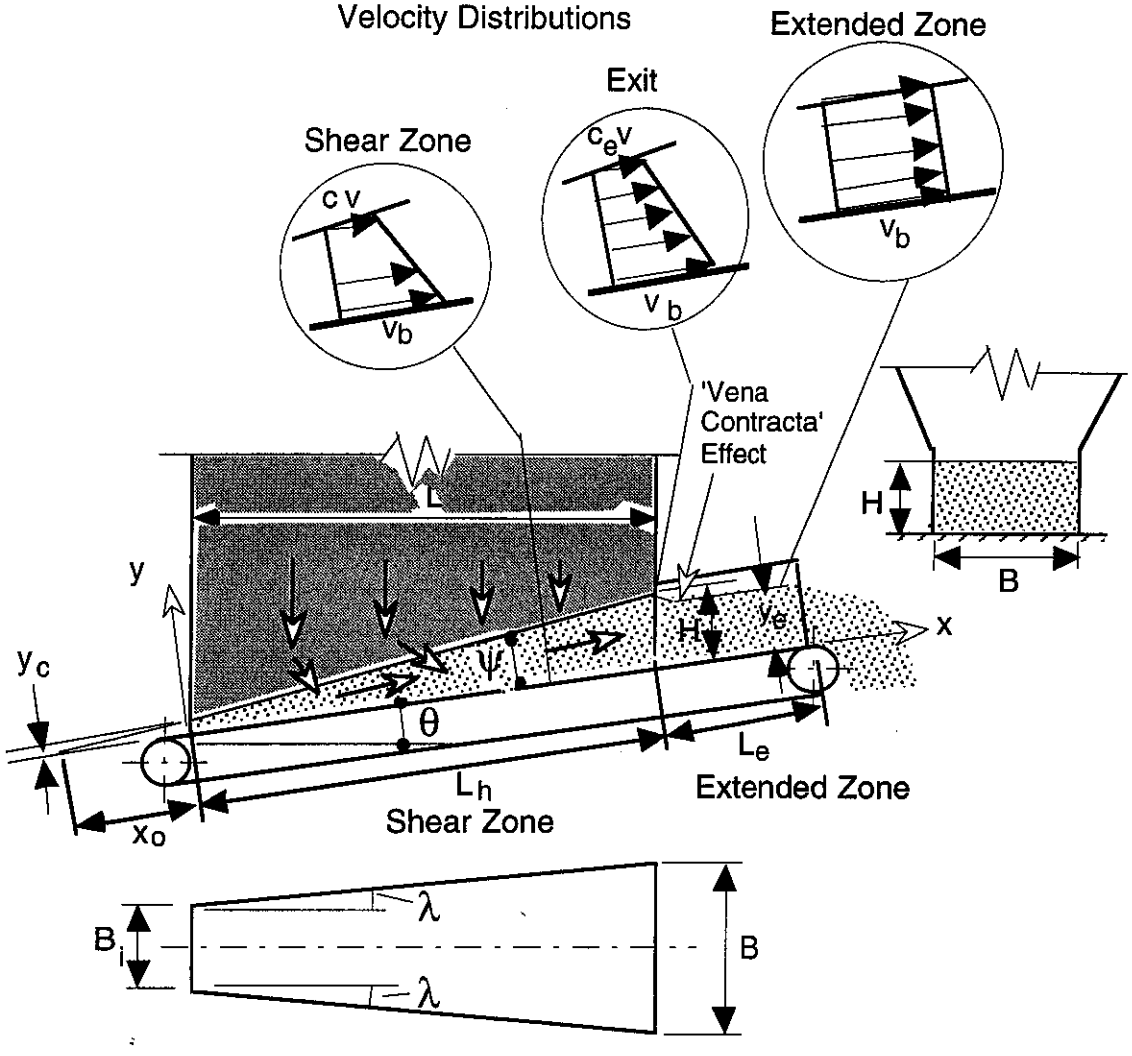

Figure 13. Belt/Apron Feeder - Assumed Shear Zone and Velocity Profile

Referring to Figure 13,

$$H = \frac{L}{\cos\theta} \tan\psi + y_c \qquad (32)$$

or

$$\frac{H}{B} = \frac{L}{B} \frac{\tan\psi}{\cos\theta} + \frac{y_c}{B} \qquad (33)$$

and the average ratio $\frac{y_c}{B}$ is

$$\frac{y_h}{B} = \frac{1}{2} \frac{L}{B} \frac{\tan\psi}{\cos\theta} + \frac{y_c}{B} \qquad (34)$$

Normally $\frac{H}{B} \leq 1.0$. For a given $\frac{H}{B}$ and $\frac{L}{B}$, the release angle is obtained from (34). That is,

$$\psi = \tan^{-1}\left[\frac{\frac{H}{B} - \frac{y_c}{B}}{\frac{L}{B}} \cos\theta\right] \qquad (35)$$

The release angles as a functions of the ratios $\frac{H}{B}$ for various $\frac{L}{B}$ ratios are given in Figure 14.

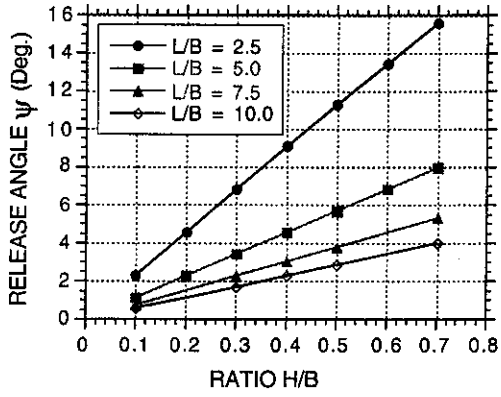

Figure 14. Variation of Release Angle with $\frac{H}{B}$ and $\frac{L}{B}$

As shown in Section 7, the release angle has a significant effect on the potential for slip to occur between the bulk solid in contact with the belt. The larger the release angle, the less likely will slip occur.

5.3 Distribution of Throughput in Feeder

Referring to Figure 12, the mass throughput of the feeder will vary along the feed zone. At any location x, the throughput $Q_m(x)$ is given by

$$Q_m(x) = \rho\, A(x)\, v_b\, \eta_V(x) \qquad (36)$$

where
$A(x)$ = Cross-sectional area at location x
v_b = Velocity of the belt or apron
ρ = Bulk density (assumed constant)
$\eta_V(x)$ = Volumetric efficiency at location x

From the geometry of Figure 13,

$$A(x) = (B_i + 2 x \tan\lambda)(y_c + x \tan\psi) \qquad (37)$$

The volumetric efficiency $\eta_V(x)$ relates the actual throughput to the maximum theoretical throughput which is the bulk solid moving forward with the belt or apron without slip. Thus $\eta_V(x)$ is given by

$$\eta_V(x) = \frac{v_f(x)}{v_b} \qquad (38)$$

where $v_f(x)$ = Average feed velocity at location x.

$$v_f(x) = (1 + C)\frac{v}{2} \qquad (39)$$

v = velocity of bulk solid at belt surface

Assuming that there is no slip at the belt surface, then $v = v_b$. Hence (50) becomes

$$v_f(x) = (1 + C)\frac{v_b}{2} \qquad (40)$$

Referring to Figure 12, it is assumed that

$$C = 1 - (1 - C_e)\left(\frac{x + x_o}{L_h + x_o}\right) \quad (41)$$

$$\eta_V(x) = 1 - \frac{(1 - C_e)\, x_o}{2\,(L_h + x_o)} - \frac{(1 - C_e)\, x}{2\,(L_h + x_o)} \quad (42)$$

Substituting for A(x) and $\eta_V(x)$ in equation (47,)

$$Q_m(x) = \rho\, v_b\, [-a_2\, a_4\, x^3 + (a_2\, a_3 - a_1\, a_4)\, x^2 + (a_1 a_3 - a_o a_4)] + \Delta Q_{mi} \quad (43)$$

where

$$a_o = y_c\, B_i$$

$$a_1 = 2\, y_c \tan\lambda + B_i \tan\psi$$

$$a_2 = 2 \tan\lambda \tan\psi$$

$$a_3 = 1 - \frac{(1 - C_e)\, x_o}{2\,(L_h + x_o)} \quad (44)$$

$$a_4 = \frac{(1 - C_e)}{2\,(L_h + x_o)}$$

$$x_o = \frac{y_c}{\tan\psi}$$

$\Delta Q_{mi} = \rho\, B_i\, y_c\, \eta_{vi}\, v_b$ = Initial throughput

5.4 Feeder Throughput

At the discharge or feed end of the hopper the throughput is given by

$$Q_m = \rho\, B\, H\, v_b\, \eta_V(L) \quad (45)$$

where $\eta_V(L) = \frac{1 + C_e}{2}$ (46)

$\eta_V(L)$ = volumetric efficiency at exit

Also, $Q_m = \rho_e\, B\, y_e\, v_b$ (47)

where ρ_e = bulk density in extended zone

It is noted that $\rho_e < \rho$ since the consolidation pressures are lower in the extended zone

Hence $y_e = H\left(\frac{1 + C_e}{2}\right)\left(\frac{\rho}{\rho_e}\right)$ (48)

The throughput is given by

$$Q_m = \rho_e\, B\, y_e\, v_b \quad (49)$$

5.5 Hopper Draw-Down

For convenience, the distribution of the throughput along the feeder, given by equation (43), may be expressed in non-dimensional form as

$$N_Q(x) = \frac{Q_m(x)}{\rho\, v_b\, B\, H} = \frac{1}{H\, B}[-a_2\, a_4\, x^3 + (a_2\, a_3 - a_1\, a_4)\, x^2 + (a_1\, a_3 - a_o\, a_4)\, x + a_o\, a_3] + \frac{B_i\, y_c\, \eta_{vi}}{B\, H\, \eta_{vL}} \quad (50)$$

$N_Q(x)$ may be normalised by choosing H = B = 1

Hence

$$N_Q(x) = \frac{Q_m(x)}{\rho\, v_b} = -a_2\, a_4\, x^3 + (a_2\, a_3 - a_1\, a_4)\, x^2 + (a_1\, a_3 - a_0\, a_4)\, x + a_0\, a_3) + \frac{B_i\, y_c\, \eta_{vi}}{\eta_{vL}} \quad (51)$$

The draw-down characteristics in the hopper are governed by the gradient of the throughput

$$Q_m'(x) = \frac{dQ_m(x)}{dx}$$

or

$$N_Q'(x) = \frac{Q_m'(x)}{\rho\, B\, H\, v_b}$$

Again normalising with H = B = 1,

$$Q_m'(x) = \rho\, v_b\, [-3\, a_2\, a_4\, x^2 + 2\, (a_2\, a_3 - a_1\, a_4)\, x + (a_1\, a_3 - a_0\, a_4)] \quad (52)$$

For best performance, uniform draw-down in the hopper is required. For this to be achieved,

$$Q_m'(x) = \frac{dQ_m(x)}{dx} \text{ constant} \quad (53)$$

or

$$N_Q'(x) = -3\, a_2\, a_4\, x^2 + 2\, (a_2\, a_3 - a_1\, a_4)\, x + (a_1\, a_3 - a_0\, a_4) \quad (54)$$

5.6 Optimum Hopper Geometry

Since equation (54) is second order, it is not possible, theoretically, to achieve uniform draw down. However, it is possible to achieve approximately constant draw-down by carefully selecting the feeder geometry. To do this, the recommended approach is to choose the feeder geometry so that the maximum value of $N_Q'(x)$ occurs at the centre of the feeder, that is, when $x = \frac{L}{2}$. In this way, distribution of $N_Q'(x)$ is approximately symmetrical.

For maximum $N_Q'(x)$, $N_Q''(x) = \frac{dN_Q'(x)}{dx} = 0$

Hence

$$N_Q''(x) = -6\, a_2\, a_4\, x + 2\, (a_2\, a_3 - a_1\, a_4) = 0$$

or

$$x = \frac{a_2\, a_3 - a_1\, a_4}{3\, a_2\, a_4}$$

Based on the assumptions embodied in Figure 17, it may be shown that the optimum hopper geometry is governed by the divergence angle l and is independent of the of the release angle y. Setting $x = \frac{L}{2}$ and substituting for a_1 to a_4 from equation (55), it may be shown that the optimum divergence angle l is given by

$$\tan \lambda = \frac{B}{2L} \left\{ \frac{1}{\frac{2}{1 - \frac{y_c}{H}} \left[\frac{1}{1 - C_e} - \frac{y_c}{H} \right] - 0.5} \right\} \quad (55)$$

Optimum values of λ computed using equation (55) are illustrated in Figures 15 and 16. In Figure 15, optimum l values are plotted against the volumetric efficiency, $\eta_V(L) = \frac{1 + C_e}{2}$ which applies at the feed end of the hopper. The plotted results apply to $\frac{L}{B} = 5.0$ and for $\frac{y_c}{H}$ values ranging from 0 to 0.5. For the theoretical special case of $C_e = 1.0$ for which $\eta_V(L) = 1.0$, the divergence angle $\lambda = 0^o$. For

the case when $C_e = 0$ for which $\eta_V(L) = 0.5$, the divergence angle $\lambda = 3.85^o$, this value of λ being the same for all clearance ratios $\frac{y_c}{B}$.

The influence of the feeder $\frac{L}{B}$ ratio on the optimum values of λ for a range of clearance ratios is illustrated in Figure 16. The optimum divergence angle λ for uniform draw-down is shown to decrease with increase in $\frac{L}{B}$ ratio, the rate of decrease being quite rapid at first but lessening as the $\frac{L}{B}$ ratio increases towards the value $\frac{L}{B} = 10$. As shown, the optimum divergence angle λ increases with decrease in clearance ratio. The volumetric efficiency variation is the same for both feeders, decreasing from 0.98 at the rear of the feeder to 0.75 At the feed end.

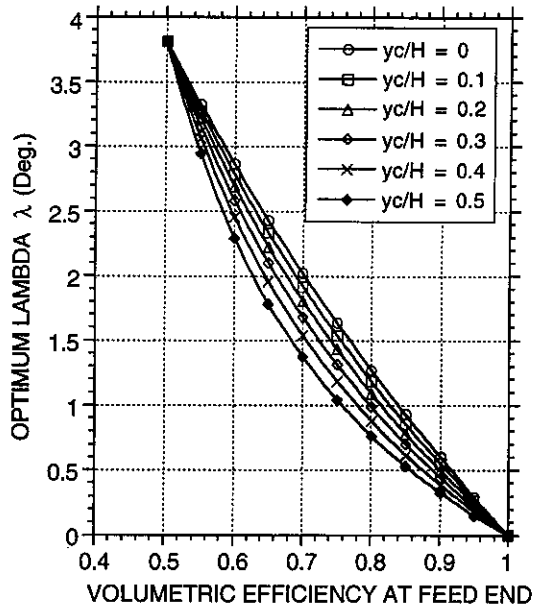

Figure 15. Optimum Divergence Angle versus Volumetric Efficiency at Feed End for a Range of Clearance Ratios

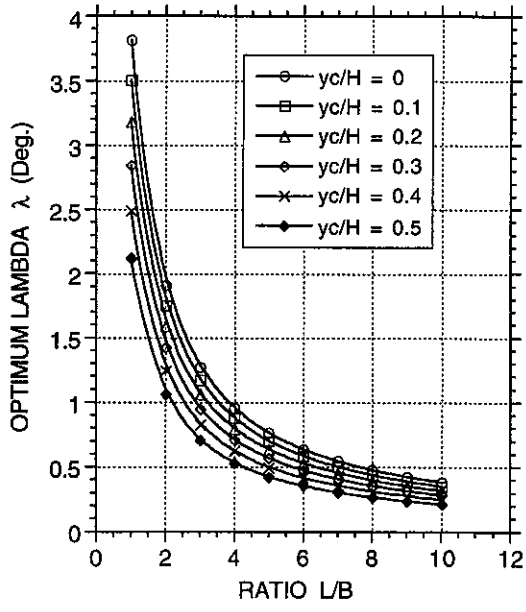

Figure 16. Optimum Divergence Angle versus L/B Ratio for a Range of Clearance Ratios
$\eta_V = 0.75$; $C_e = 0.5$

5.7 Belt Feeder Example

Figure 17 shows the volumetric efficiency $h_V(x)$, throughput parameter $N_Q(x)$ and gradient $N_Q'(x)$ for two feeder geometries for the case of $\frac{L}{B}$ = 5 and C_e = 0.5. The full lines for $N_Q(x)$ and $N_Q'(x)$ correspond to the optimum divergence angle $\lambda = 1.54^o$ and as shown, the gradient $N_Q'(x)$ is virtually constant indicating uniform draw-down in the hopper.

For comparison purposes, the performance of a feeder having the same feed rate as the optimum feeder but with a larger divergence angle of 3^o is also presented. The relevant graphs are shown by dotted lines. As shown, the gradient $N_Q'(x)$ for this case increases toward the feed end which indicates that the hopper will draw down preferentially from the front.

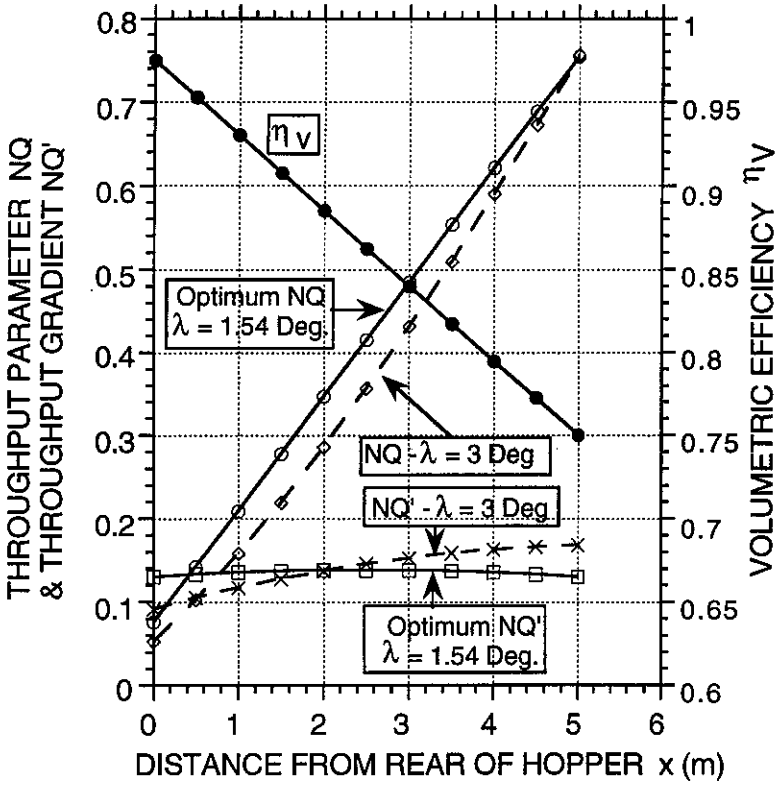

Figure 17. Throughput Characteristics of Belt Feeder - η_V = 0.75 C_e = 0.5
Case 1: Optimum $\lambda = 1.54^o$ Case 2: $\lambda = 3^o$

6. DRIVE RESISTANCES - BELT AND APRON FEEDERS

The general layout of a belt or apron feeder is shown in Figure 18.

The various resistances to be overcome, which are analysed in Refs.[7,8], are:

(i) Force to shear bulk solid

(ii) Force to overcome skirtplate friction in the hopper zone and in the extended zone beyond the hopper

(iii) Force to move belt or apron against support idlers

(iv) Force to elevate the bulk solid

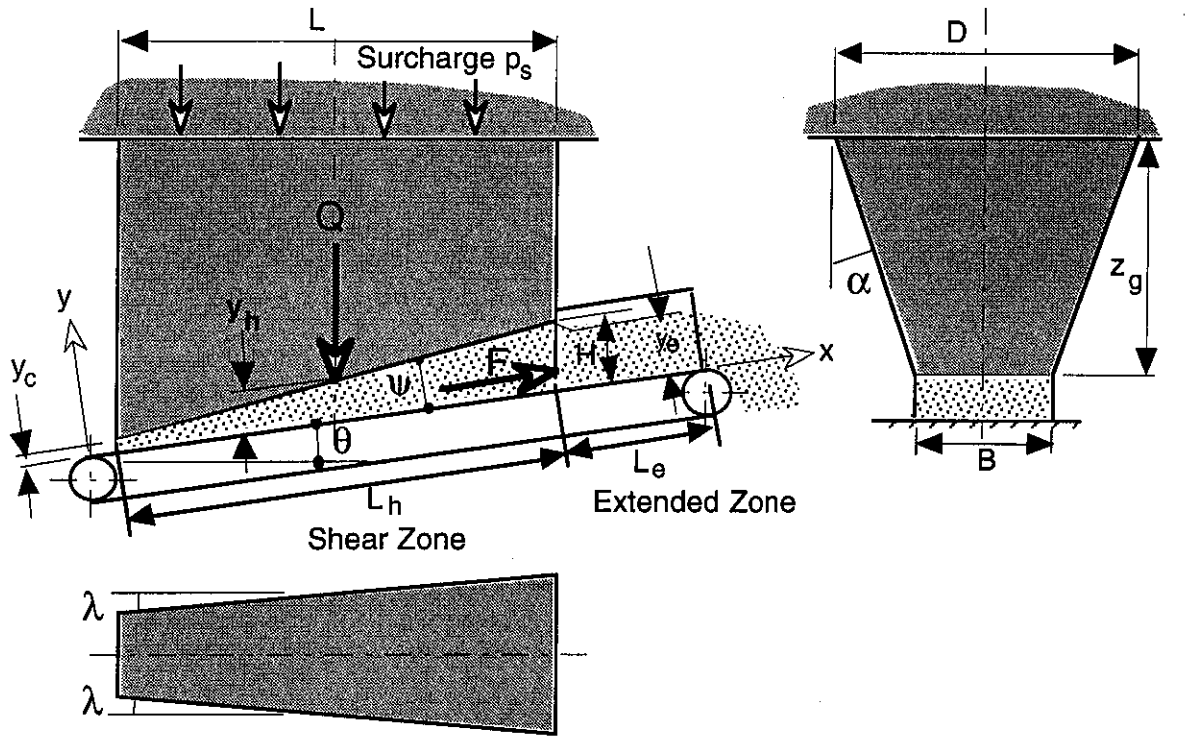

Figure 18. Hopper Geometry for Feeder Load Determination

6.1 Tangential Load

The forces acting in the feed zone are illustrated diagrammatically in Figure 18. The tangential force to shear the material may be computed from

$$F = \mu_E \, Q \qquad (56)$$

where μ_E = Equivalent friction coefficient

The following friction coefficients have been suggested:
Reisner: $\mu_E = 0.4$, Jenike: $\mu_E = 0.45$
The internal friction coefficient at the surface of the shear plane is normally taken to be

$$\mu_S = \sin \delta \qquad (57)$$

Allowing for the diverging wedge shape of the assumed shear zone, a simple, empirical expression for the equivalent friction coefficient μ_E is

$$\mu_E = K \sin \delta. \qquad (58)$$

Experience has shown that K = 0.8 gives a satisfactory prediction in most cases.

However an alternative expression based on the geometry of the feed zone may be determined as indicated in Ref.[9]

$$\mu_E = \frac{\mu_S \cos \psi - \sin \psi}{\cos(\theta + \psi)[\,1 + \mu_S \, \mu_{Wi}] + \sin(\theta + \psi)[\mu_S - \mu_{Wi}]} \qquad (59)$$

where
θ = feeder inclination angle
ψ = release angle
μ_S = friction at shear surface
μ_{Wi} = end wall friction

In effect, μ_{Wi} serves to reduce the load Q acting on the feeder.

The more conservative approach is to assume that $\mu_{wi} = 0$. Hence,

$$\mu_E = \frac{\mu_s \cos\psi - \sin\psi}{\cos(\theta + \psi) + \mu_s \sin(\theta + \psi)} \qquad (60)$$

By way of example, a set of design curves based on equation (60) is shown in Figure 19.

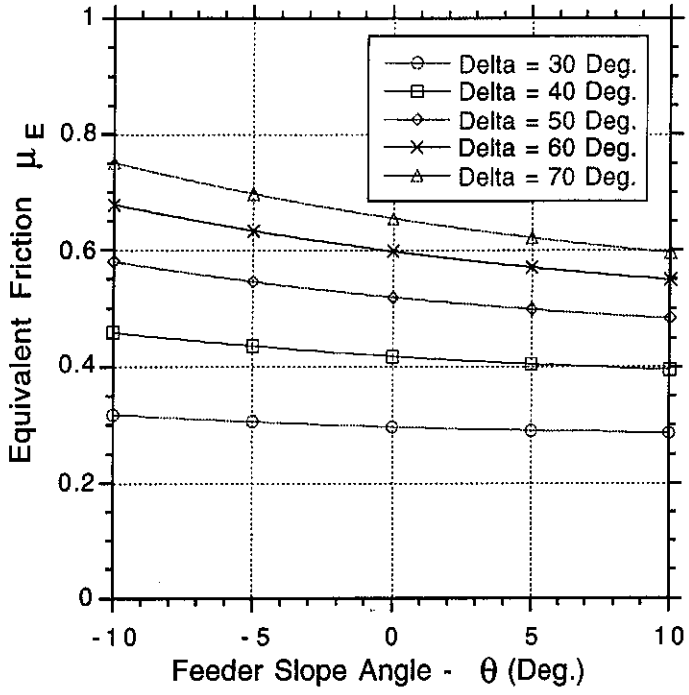

Figure 19. Equivalent Friction for Belt and Apron Feeder - $\psi = 10^o$

6.2 Skirtplate Resistance

Assuming steady flow, the skirtplate resistance is determined for the hopper and extended sections (see Figure 18). The pressure distributions for the skirtplate sections are assumed to be hydrostatic as illustrated in Figure 20.

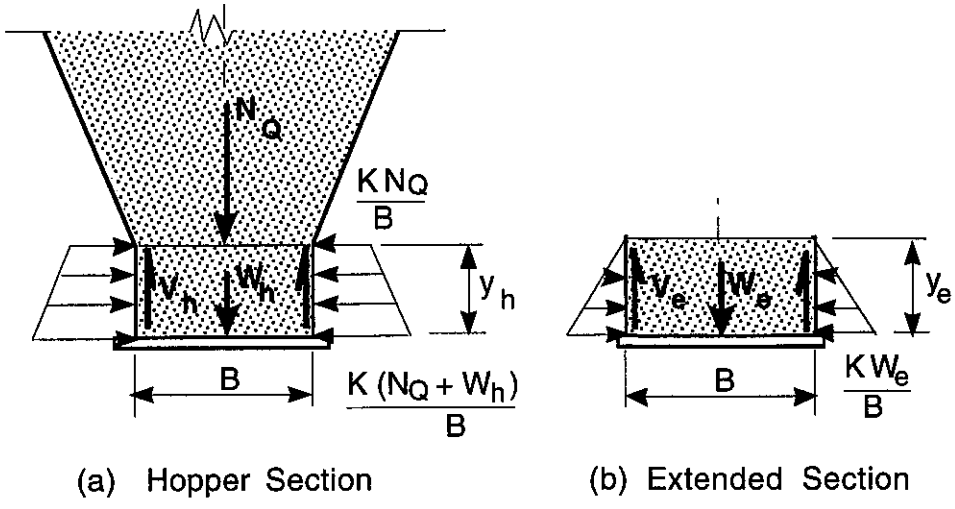

Figure 20. Pressure Distributions for Skirtplate Zones

Neglecting the vertical support V_h and V_e due to the skirtplates, the skirtplate resistance is given by

(i) Hopper Section

$$F_{sph} = \mu_{sp} K_v \left(2 N_Q + \rho g B L_h y_h \right) \frac{y_h}{B} \quad (61)$$

(ii) Extended Section (Section beyond hopper)

$$F_{spe} = \mu_{sph} K_v \rho g L_e y_e^2 \quad (62)$$

where N_Q = Feeder load normal to belt or apron surface = Q cos q
ρ = Bulk density
y_h = Average height of material against skirtplates for hopper section
y_e = Average height of material against skirtplates for extended section
K_v = Ratio of lateral to vertical pressure at skirtplates
g = Acceleration due to gravity = 9.81 (m/s^2)
B = Width between skirtplates
μ_{sph} = Equivalent skirtplate friction coefficient
L_e = Length of skirtplates for extended section

It should be noted that in the hopper zone, the skirtplates are diverging. Hence the frictional resistance will be less than in the case of parallel skirts. Referring Figure 20, μ_{sph} may be estimated from

$$\mu_{sph} = \frac{\mu_{sp} - \tan \lambda}{1 + \mu_{sp} \tan \lambda} \quad (63)$$

where λ = Half divergence angle of skirtplates
μ_{sp} = Friction coefficient for skirtplates

The pressure ratio K_v is such that $0.4 \leq K_v \leq 1.0$. The lower limit may be approached for the static case and the upper limit for steady flow. In the case of slow feed velocities, as in the case of apron feeders, the value of K_v for flow may be in the middle range.

6.3 Load Slope Resistance

$$F_{slope} = (W + W_e) \sin \theta \quad (64)$$

W = Weight of material in skirtplate zone of hopper
W_e = Weight of material in extended skirtplate zone of hopper

6.4 Belt or Apron Load Resistance

(i) Hopper Section

$$F_{bh} = (N_Q + \rho g B L y_h) y_h \mu_b \quad (65)$$

(ii) Extended Section

$$F_{be} = \rho g B L_e y_e \mu_b \quad (66)$$

where μ_b = Idler friction.

6.5 Empty Belt or Apron Resistance

$$F_b = w_b L_B \mu_b \quad (67)$$

where w_b = Belt or apron weight per unit length
L_B = Total length of belt $\geq 2 (L_h + L_e)$

6.6 Force to Accelerate Material onto Belt or Apron

$$F_A = Q_m v_b \tag{68}$$

where Q_m = Mass flow rate
v_b = Belt or apron speed

It is assumed that

$$Q_m = \rho B y_e v_b \tag{69}$$

Usually the force F_A is negligible.

It should be noted that for good performance, belt and apron speeds should be kept low. Generally $v_b \leq 0.5$ m/s.

7.7 Drive Powers

The foregoing loads and resistances are determined for the initial and flow conditions using the appropriate values of the variables involved. The power is computed from

$$P = (\Sigma \text{ Resistances}) \frac{v_b}{\eta} \tag{70}$$

where η = efficiency and v_b = average belt or apron speed. For start-up, v_b may be approximated as half the actual speed. For the flow condition, v_b will be the actual belt or apron speed during running.

7. CONDITION FOR NON-SLIP

The condition for non-slip between the belt and bulk solid under steady motion can be determined as follows:

$$\mu_B (Q_f + W_T) \geq (F_f + F_{sp} + F_{slope} + F_a) \tag{71}$$

where

$$\mu_B = \mu_b \cos\theta - \sin\theta \tag{72}$$

μ_b = Coefficient of friction between belt or apron and bulk solid
Q_f = Flow surcharge load on shear plane at hopper outlet
W_T = Total weight of bulk material in skirtplate zones
F_f = Force to shear material at hopper outlet
F_{sp} = Skirtplate resistance.

A more detailed analysis of the condition for non slip is given in Ref.[8] The essential relationships are summarised below.

The general relationship for no slip is shown to be

$$\mu_b = \tan\phi_b \geq \frac{R \sin(\phi_s - \psi) + W \sin\theta + F_{sp} + F_a}{R \cos(\phi_s - \psi) + W \cos\theta} \tag{73}$$

or

$$\mu_b = \tan\phi_b \geq \frac{F_{sb} + W \sin\theta + F_{sp} + F_a}{F_{sb} \cos(\phi_s - \psi) + W \cos\theta} \tag{74}$$

where $F_{sb} = \mu_E Q$

7.1 Case When $F_a \approx 0$ and End Wall Friction ≈ 0

In most cases, the belt or apron speed is low enough to render $F_a \approx 0$.

$$\mu_b = \tan \phi_b \geq \frac{R \sin(\phi_s - \psi) + W \sin \theta + F_{sp}}{R \cos(\phi_s - \psi) + W \cos \theta} \quad (75)$$

Expressing R in terms of the feeder load Q leads to

$$\mu_b \geq \frac{Q \sin(\phi_s - \psi) + \beta (W \sin \theta + F_{sp})}{Q \cos(\phi_s - \psi) + \beta W \cos \theta} \quad (76)$$

where $\beta = \cos(\phi_s - \theta - \psi)$ (77)

θ = feeder slope
ψ = release angle
ϕ_s = friction angle at shear surface

Skirtplate resistance

$$F_{sp} = F_{sph} + F_{spe}$$

$$F_{sp} = K_v \cos \theta \left[\mu_{sph} \frac{y_h}{B} (2 Q + W) + \mu_{sp} W_e \frac{y_e}{B}\right] \quad (78)$$

where W = Weight of bulk solid in shear zone of hopper
W_e = Weight of bulk solid in extended zone

Generalised Equation for μ_b

Let $C_Q = \frac{W}{Q}$ (79)

and $C_{Qe} = \frac{W_e}{Q}$ (80)

From Figure 20, for a small clearance y_c, $\frac{y_h}{B} \approx \frac{y_e}{2B}$

Hence, equation (78) becomes

$$\mu_b = \frac{\sin(\phi_s - \psi) + \beta\{C_Q \sin \theta + K_v \cos \theta \frac{y_e}{B} [0.5 m_{sph} (2 + C_Q) + \mu_{sp} C_{Qe}]\}}{\cos(\phi_s - \psi) + \beta C_Q \cos \theta} \quad (81)$$

7.2 NUMERICAL EXAMPLE

Figure 21 illustrates the minimum belt /apron friction angle as a function of release angle to prevent slip for the case when

$\frac{L}{B} = 5$; $\frac{y_c}{B} \approx 0$; $\delta = 50^o$; $\mu_s = \sin \delta = 0.76$; $\phi_s = \tan^{-1} 0.76 = 37^o$; $C = C_e = 0.05$

The graphs have been plotted for the feeder slope angles, -10^o, 0^o, and 10^o.

In this case, $\eta_v(L) = \frac{(1 + C_e)}{2}$ and $C_e = 1 - 0.5 \frac{H}{B}$

As indicated, the minimum belt friction angle ϕ_b is less sensitive to changes in feeder slope, but is more sensitive to the release angle ψ, decreasing with increase in ψ as indicated.

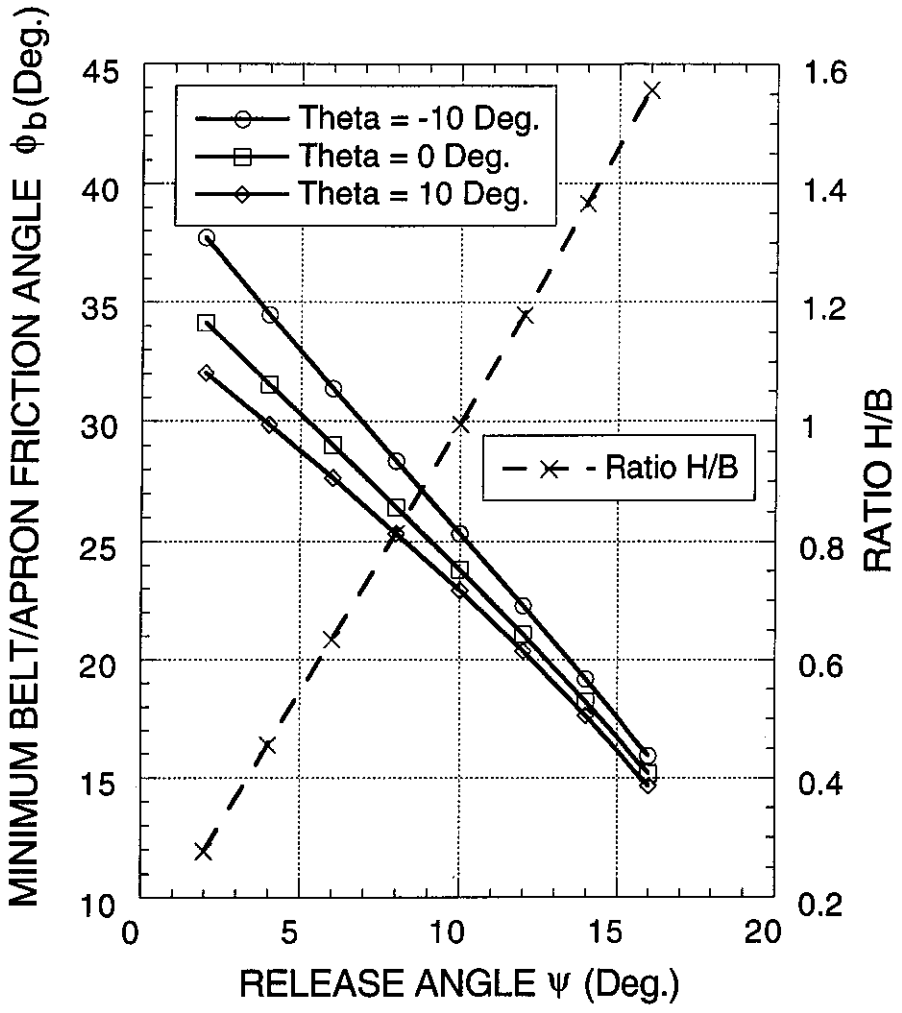

Figure 21. Minimum Belt/Apron Friction Angle to Prevent Slip

$\frac{L}{B} = 5$; $\frac{y_c}{B} = 0.1$; $\delta = 50^o$; $\mu_s = \sin\delta = 0.76$; $\phi_s = \tan^{-1} 0.76 = 37^o$; $C_Q = C_{Qe} = 0.05$

Optimum $\lambda = 1.54^o$; $C_e = 0.5$

8. CONTROLLING FEEDER LOADS AND POWER

The loads on feeders and the torque during start-up may be controlled by ensuring that an arched stress field fully or partially exists in the hopper just prior to starting. This may be achieved by such procedures as:

- Cushioning in the hopper, that is leaving a quantity of material in the hopper as buffer storage.
- Raising the feeder up against the hopper bottom during filling and then lowering the feeder to the operating condition prior to starting. In this way an arched stress field may be partially established.
- Starting the feeder under the empty hopper before filling commences.
- Using transverse, triangular-shaped inserts

8.1 Load Cushioning

The high initial loads which may act on feeders are a matter of some concern and, where possible, steps should be taken to reduce the magnitude of these loads. Bearing in mind the need to maintain a fully active hopper outlet, it is possible to control or limit the load on the feeder by always retaining a

cushion of material in the hopper. The advantage of this practice with respect to feeder loads is illustrated in Figure 22.

From a practical point of view, the practice of maintaining a cushion of material in the hopper is most desirable in order to protect the hopper surface from impact damage during filling. However there is a further advantage; the material left in the hopper as a cushion, having previously been in motion, will preserve the arched stress field. This will provide a surcharge load on the arch field, but the load at the outlet will be of lower order than if the bin is totally filled from the empty condition. From Figure 22, the substantial reduction in the initial feeder load as the cushion head increases is clearly evident.

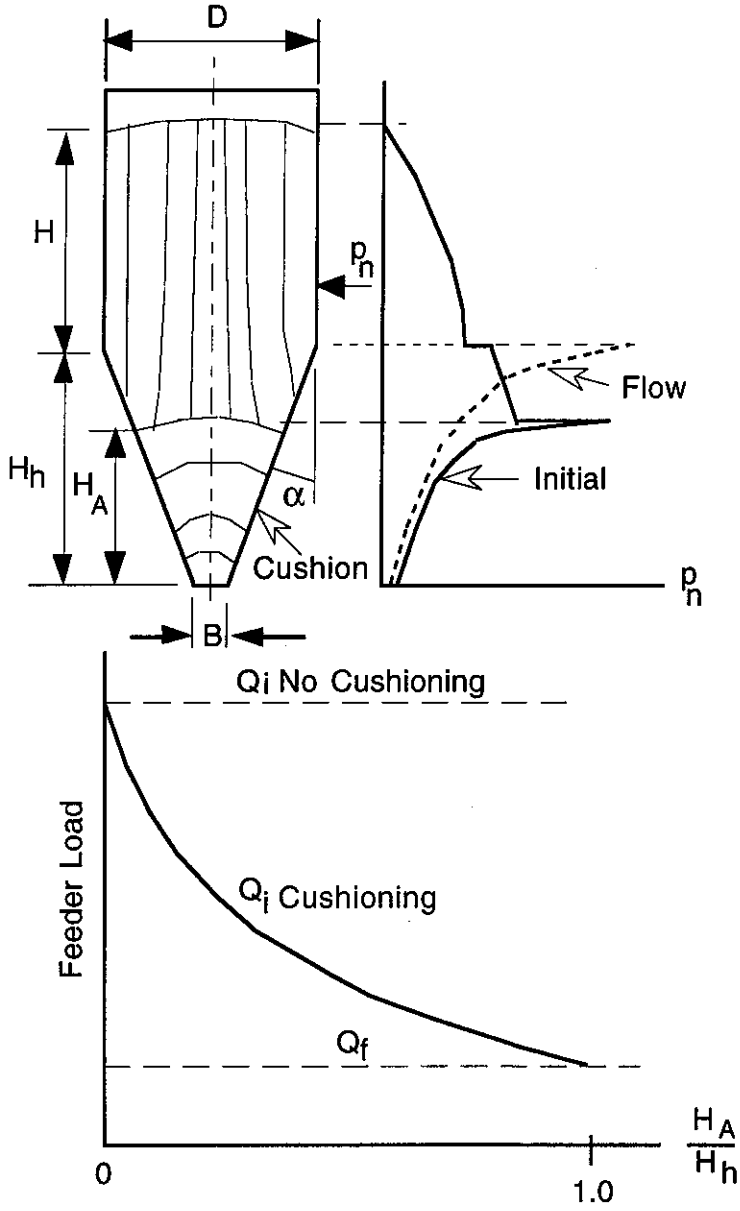

Figure 22. Cushioning in the Hopper to Control Feeder Loads

8.2 Raising and Lowering the Feeder

It needs to be noted that the choice of mounting arrangement for a feeder can assist in generating a preliminary arched stress field near the outlet sufficient to moderate both the initial feeder load and starting power. In the case of vibratory feeders, for example, it is common to suspend the feeders on springs supported off the bin structure as illustrated in Figure 23. The initial deflection of the springs during filling of the bin can assist in generating an arched pressure field near the outlet and reduce the initial load. For a belt feeder, it may be thought useful to incorporate a jacking arrangement to lift the feeder up against the bottom of the hopper during filling. Before starting, the feeder is released to its operating position sufficient to cause some movement of the bulk solid in order to generate a cushion

effect. The use of a slide gate or valve above the feeder is another way of limiting the initial load and power. The gate is closed during filling and opened after the feeder has been started.

For 'emergency' purposes, the provision of jacking screws as illustrated in Figure 23 can be used to lower the feeder should a peaked stress field be established on filling and there is insufficient power to start the feeder. Lowering the feeder can induce, either fully or partially, an arched stress field and allow the feeder to be started.

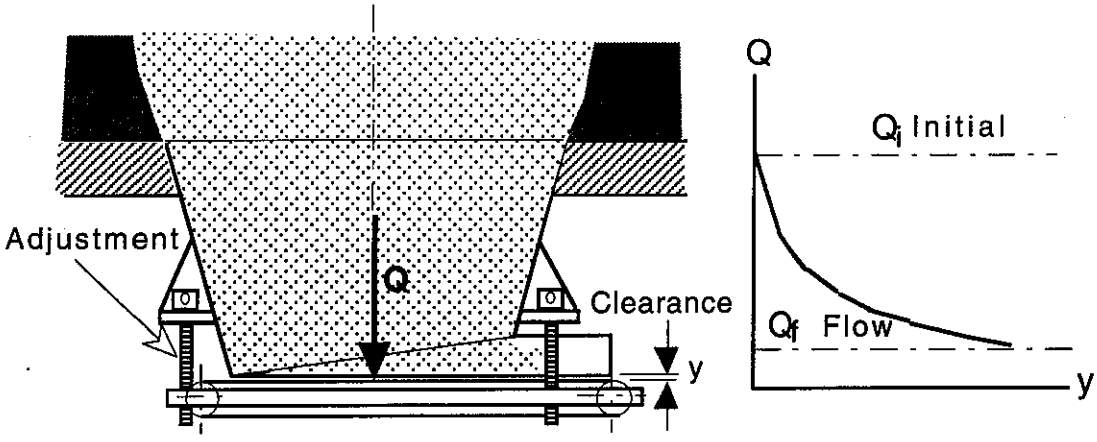

Figure 23. Use of Jacking Screws to Lower the Feeder

8.3 Starting the Feeder Before Filling Commences

Starting the feeder under the empty hopper before filling commences can also allow the arched stress field to be established. Once the hopper is filled, the feeder may be stopped if desired and the filling process continued.

8.4 Use of Transverse Inserts

In the case of feeders employing long opening slots, the use of transverse inserts can assist in the reducing the initial load, as well as promoting uniform draw of bulk solid from the hopper along the length of the feeder. The used of transverse inserts is illustrated in Figure 24. A difficulty associated with long narrow slots is the limitation in release angles which can give rise to belt slip.

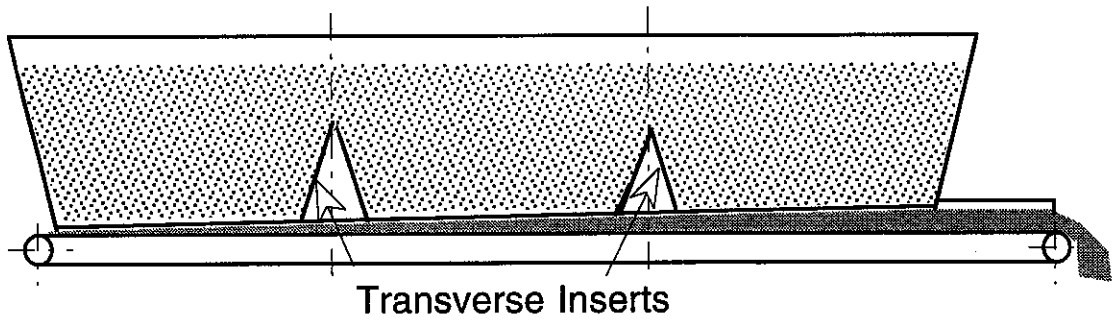

Figure 24. Use of Transverse Inserts to Control both Load and Flow Pattern

10. SURCHARGE LOAD ON FEEDER - INITIAL FILLING CONDITION

The computation of the initial vertical load acting on a feeder requires a knowledge of the surcharge pressure p_s acting at the transition of the feed hopper. It is to be noted the flow load acting on a feeder is independent of the surcharge head. The determination of the initial surcharge pressure p_s depends on the type of storage system employed. The following cases are considered:

9.1 Mass-Flow and Expanded Flow Bins

Referring to Figure 25, the surcharge head is given by the Janssen equation:

$$h_c = \frac{R}{K_j \tan\phi} \left[1 - e^{-K_j \tan\phi \, H/R} \right] + h_s \, e^{-K_j \tan\phi \, H/R} \qquad (82)$$

The corresponding pressure p_c is

$$p_c = \gamma h_c \qquad (83)$$

where R = 'Hydraulic' Radius defined as

$$R = \frac{D}{2\,(1 + m_c)} \qquad (84)$$

m_c = 0 for long rectangular cylinder
m_c = 1 for square or circular cylinder

H = Height of bulk solid in contact with cylinder walls
$K_j = p_n/p_v$ for cylinder. Normally K_j = 0.4
ϕ = Wall friction angle for cylinder

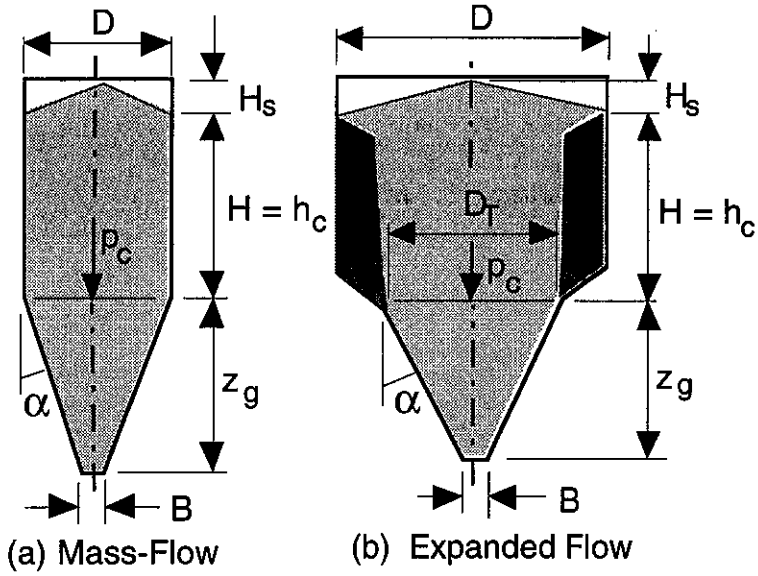

Figure 25. Mass-Flow and Expanded-Flow Bins

The effective surcharge head is given by

$$h_s = \frac{H_s}{m_s + 2} \qquad (85)$$

where H_s = Surcharge head
m_s = 1 for conical surcharge
m_s = 0 for triangular surcharge

9.2 Gravity Reclaim Stockpile

The use of mass-flow reclaim hoppers and feeders under stockpiles is illustrated in Figure 26. The initial load Q_i on the reclaim feeder is dependent on the effective surcharge head, while the flow load Q_f is independent of the head as illustrated.

The determination of surcharge head and pressure in the case of stockpiles is somewhat uncertain owing to the significant variations that can occur in the consolidation conditions existing within the stored bulk solid. The state of consolidation of the bulk solid is influenced by such factors as

- Stockpile management and loading history
- Loading and unloading cycle times and length of undisturbed storage time
- Variations in moisture content
- Degree of segregation
- Variations in the quality of bulk solid over long periods of time
- Compaction effects of heavy mobile equipment that may operate on the surface of the stockpile

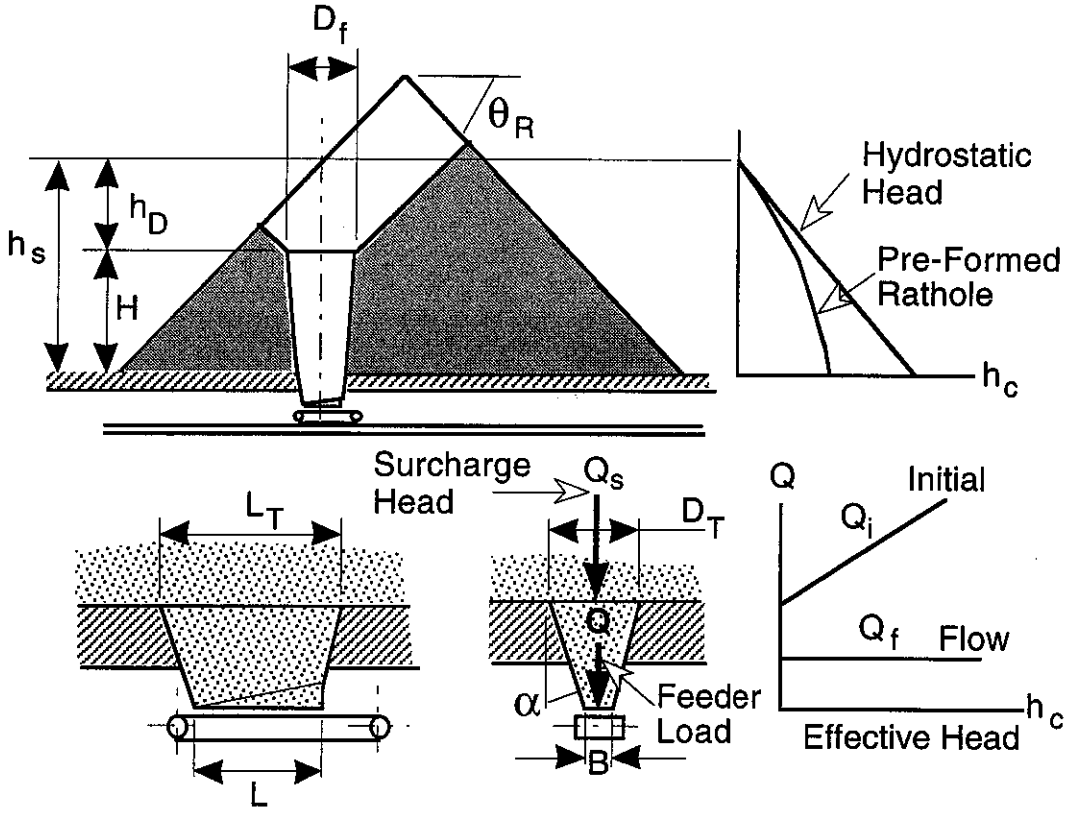

Figure 26. Gravity Reclaim Stockpile

As a result of recent research and field studies, procedures are recommended for the following two cases:

(a) Case 1 - Freshly Formed or Uniformly Consolidated Stockpile in which withdrawal occurs at regular intervals.

$$h_c = H \qquad (86)$$

That is the effective head is equal to the actual head. This is the most conservative solution.

In some cases, a less conservative solution may be applied through the use of the Rankine pressure or head. That is

$$h_c = H \cos \phi_r \qquad (87)$$

where ϕ_r = Angle of repose

(b) Case 2 - Well Consolidated Stockpile in which the rathole above the feeder is well formed and stable.

In this case the rathole serves as a pseudo-bin and the effective head may be estimated using the Janssen equation following the procedures described in Section 9.1 for an expanded flow bin. In this case the cylinder diameter is the actual rathole diameter D_f, and the wall friction angle becomes the static angle of internal friction ϕ_f. In reality, the shape of ratholes is not cylindrical so the Janssen approach is an approximation.

10. FEEDER LOADS FOR FUNNEL-FLOW

In the case of feeders under funnel-flow bins, the load Q on the feeder will be the total effective head of bulk solid computed on the basis of Janssen or the 'hydrostatic' head as may be relevant. The existence of a 'flow stress field' situation as applies under mass-flow does not apply in the funnel-flow case.

11. FEEDING ONTO BELT CONVEYORS

The efficient operation of belt conveyors depends on a many factors, not the least of which is effective loading or feeding of bulk solids onto the belts at the feed or intake end. The fact that belt or apron feeders are normally limited to speeds of up to 0.5 m/s, the bulk solid has to be accelerated to enter the conveyor belt at a speed matching, as close as possible, that of the belt. Two methods of achieving this are possible

- the use of accelerator belts
- employing gravity to accelerate the bulk solid in association with a feed chute

Accelerator belts are the more costly of the above two methods and are subject to significant belt wear. Gravity feed chutes, which require the necessary head room to accelerate the bulk solid to belt speed, are the better option. The objectives of chute design are to ensure streamlined flow without spillage and with minimum chute and belt wear. This, in turn, requires the correct choice of lining materials to suit the bulk solid and chute geometry.

11.1 Aspects of Chute Design

(a) Free Fall of Bulk Solid

Figure 28 illustrates the application of a gravity feed chute to direct the discharge from a belt or apron feeder to a conveyor belt. The bulk solid is assumed to fall vertically through a height 'h' before making contact with the curved section of the feed chute. Since, normally, the belt or apron speed $v_f \leq 0.5$ m/s, the velocity of impact v_i with the curved section of the feed chute will be, essentially, in the vertical direction.

For the free fall section, the velocity v_i may be estimated from

$$v_i = \sqrt{v_{fo}^2 + 2\,g\,h} \qquad (88)$$

Equation (88) neglects air resistance, which in the case of a chute, is likely to be small. If air resistance is taken into account, the relationship between height of drop and velocity v_i (Figure 28) is,

$$h = \frac{v_\infty^2}{g} \log_e \left[\frac{1 - \frac{v_{fo}}{v_\infty}}{1 - \frac{v_i}{v_\infty}} \right] - \left(\frac{v_i - v_o}{g} \right) v_\infty \qquad (89)$$

where v_∞ = terminal velocity
v_{fo} = vertical component of velocity of bulk solid discharging from feeder
v_i = velocity corresponding to drop height 'h' at point of impact with chute.

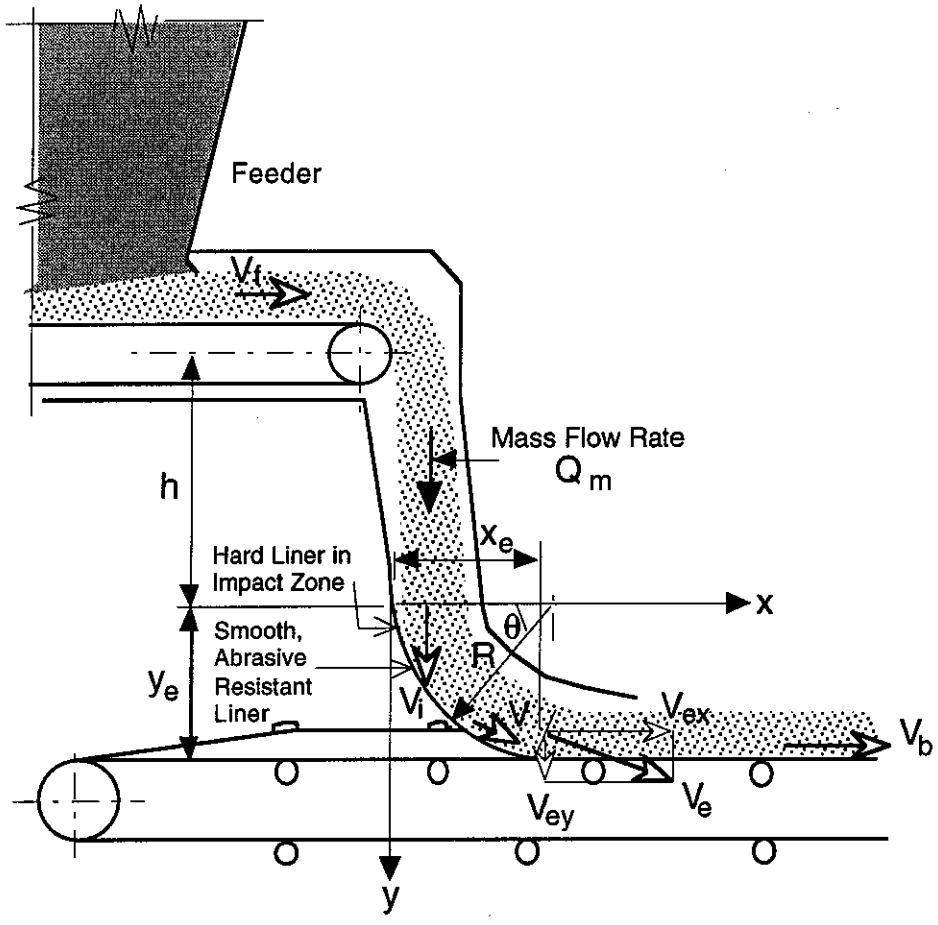

Figure 28. Feed Chute Configuration

(b) Flow of Bulk Solid around Curved Chute

If the curved section of the chute is of constant radius R, the velocity at any location θ may be computed from the equation given below (Ref.[9]),

$$v = \sqrt{\frac{2\,g\,R}{4\,\mu_e^2 + 1}\left[\sin\theta\,(1 - 2\,\mu_e^2) + 3\,\mu_e\cos\theta\right] + e^{-2\,\mu_e\,\theta}\left[v_i^2 - \frac{6\,\mu_e\,R\,g}{4\,\mu_e^2 + 1}\right]} \qquad (90)$$

where μ_e = equivalent friction which takes into account the friction coefficient between the bulk solid and the chute surface and the chute cross-section.

The objectives are

- to match the horizontal component of the exit velocity v_{ex} as close as possible to the belt speed
- to reduce the vertical component of the exit velocity v_{ey} so that abrasive wear due to impact may be kept within acceptable limits.

The abrasive wear of the belt may be estimated as follows:

Impact pressure $p_{vi} = \rho\, v_{ey}^2$ (kPa)

where ρ = bulk density, t/m^3

v_{ey} = vertical component of the exit velocity, m/s

Abrasive wear $W_a = \mu_b \rho v_{ey}^2 (v_b - v_{ex})$ (91)

Where μ_b = friction coefficient between the bulk solid and conveyor belt

Apart from minimising belt wear, it is also important to minimise the wear of the chute lining surfaces. As illustrated in Figure 28, the curved chute is divided into two zones, the impact region where the low impact angles require the use of a hard lining surface, and the other, the streamlined flow region where low friction and low abrasive wear is a necessity.

11.2 Example

The following example is considered:

Referring to Figure 28, Q_m = 1000 t/h, h = 1.0 m, R = 3.0 m, ρ = 1 t/m^3. It is assumed that μ_e = 0.5

Based on a terminal velocity v_∞ = 30 m/s and zero initial velocity, v_{fo} = 0, the impact velocity is estimated to be, v_i = 4.4 m/s. Utilising equation (90), the variation in velocity 'v' around the chute may be computed as well as the velocity components v_{ex} and v_{ey}. These velocities are plotted, together with the chute profile in Figure 29.

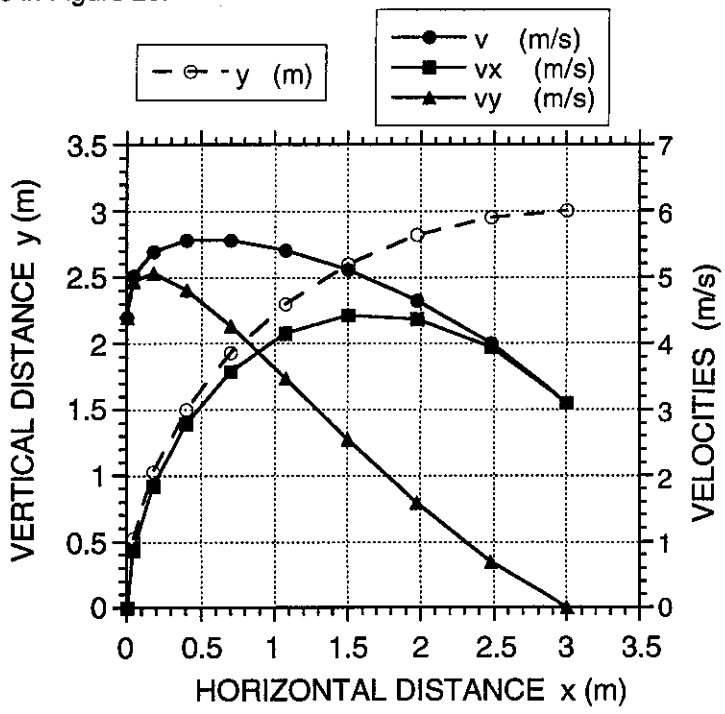

Figure Curved Chute Performance

R = 3 m; v_i = 4.4 m/s ; μ_e = 0.5; Q_m= 1000 t/h; ρ = 1 t/m^3

The maximum velocities are

v_{max} = 5.56 m/s at $\theta = 40^o$

$v_{x,max}$ = 4.43 m/s at $\theta = 60^o$

$v_{y,max}$ = 5.06 m/s at $\theta = 20^o$

Of particular interest is $v_{ex} = v_{x,max}$ = 4.43 m/s for $\theta = 60^o$, the corresponding values of x and y being x_e = 1.5 m and y_e = 2.6 m. The total height of drop = h + y_e = 3.6 m

Also, the corresponding value of $v_y = v_{ey}$ = 2.56 m/s.

Assuming the belt speed is v_b = 4.5 m/s and μ_b = 0.6

From equation (89), the abrasive wear factor W_a = 0.6 x 1.0 x 2.56^2 x (4.5 - 4.43) = 0.28 kPa m/s. Note that it is not necessary to choose the condition for maximum v_{ex}. Lower values of W_a may be obtained by choosing other values of v_{ex} and v_{ey}.

It needs to be noted that, for a given head height, best performance is generally obtained by selecting a large radius 'R' relative to the height 'h'.

12. CONCLUDING REMARKS

The concepts of feeder design in relation to loading of bulk solids onto belt conveyors has been presented. The need for feeders and mass-flow hoppers to be designed as an integral unit to promote uniform feed has been emphasised and the general expressions for feeder loads have been presented. Recommendations for optimising the geometry of the hopper and feeder interface have been given.

Taking account of the hopper and feeder geometry, together with the properties of the bulk solid, the procedures for determining the tangential driving loads and corresponding drive powers have been discussed. The significance of the arched stress field in the hopper for controlling feeder loads has been explained. The estimation of loads on feeders used in conjunction with funnel-flow, expanded-flow bins and gravity reclaim stockpiles has been outlined. The design of feed chutes for directing the flow of bulk solids from the feeder discharge onto conveyor belts is briefly reviewed.

13. REFERENCES

1. Reisner, W. and Eisenhart Rothe, M.v. "Bins and Bunkers for Handling Bulk Materials", Trans Tech Publications, Germany, 1971

2. Roberts A.W., Ooms M. and Manjunath K.S. "Feeder Load and Power Requirements in the Controlled Gravity Flow of Bulk Solids from Mass-Flow Bins" Trans. I.E.Aust., Mechanical Engineering, Vol. ME9, No.1, April 1984 (pp. 49 -61).

3. Manjunath K.S. and Roberts, A.W. "Wall Pressure-Feeder Load Interactions in Mass-Flow Hopper/Feeder Combinations". Intl. Jnl. of Bulk Solids Handling, Part I- Vol 6 No. 4, August 1986. Part II - Vol. 6 No.5 October 1986.

4. Arnold, P.C., McLean, A.G. and Roberts, A.W. "Bulk Solids: Storage, Flow and Handling", TUNRA, The University of Newcastle, 1982

5. Roberts, A.W. "Basic Principles of Bulk Solids Storage, Flow and Handling", Institute for Bulk Materials Handling Research, The University of Newcastle, Australia, 1992.

6. Schulze, D. and Schwedes, J. "Bulk Solids Flow in the Hopper/Feeder Interface", Proc. Symposium on Reliabler Flow of Particulate Solids (RELPOWFLO II), Oslo, Norway, 23-25 August, 1993

7. Rademacher, F.J.C. "Reclaim Power and Geometry of Bin Interfaces in Belt and Apron Feeders". Intl. Jnl. of Bulk Solids Handling, Vol. 2, No. 2, June 1982

8. Roberts, A.W. "Feeding of Bulk Solids - Design Considerations, Loads and Power". Course notes, Bulk Solids Handling (Systems and Design). Centre for Bulk SAolids and Particuate Technologies, The University of Newcastle, May, 1997.

9. Roberts, A.W. "An Investigation of the Gravity Flow of Non-cohesive Granular Materials through Discharge Chutes". Transactions ASME, Jnl. of Engng. in Industry, Vol 91, Series B, No. 2, May 1969.